International Journal of Power Electronics and Drive System (IJPEDS)
Vol. 16, No. 4, December 2025, pp. 2453~2463
ISSN: 2088-8694, DOI: 10.11591/ijpeds.v16.i4.pp2453-2463

Design and simulation of inductive power transfer system using hybrid compensation topologies

Noor Sami, Harith Al-Badrani
Department of Electronic Engineering, College of Electronic Engineering, Ninevah University, Mosul, Iraq

Article Info

Article history:

Received Jul 22, 2025
Revised Sep 28, 2025
Accepted Oct 3, 2025

Keywords:

Compensation topologies
Electric vehicle
Inductive power transfer
LCC/LCC compensation
LCC/S compensation
Wireless power transfer

ABSTRACT

This research addresses the principle of wireless power transfer (WPT). The system is primarily based on inductive power transfer (IPT). IPT is a recent technology that enables electrical power to be transferred between two coils via a magnetic field without the need for physical conductors. This method is particularly useful in applications where conventional wires cannot be used, such as biomedical implants, electric vehicles, and consumer electronics. Existing advances in system design, magnetic materials, and compensation topologies have significantly improved system performance and expanded their application range. Main challenges in IPT systems include improving efficiency and transmission distance. Hybrid compensation techniques in IPT systems have emerged as a promising solution to enhance system stability and power transfer efficiency under varying load conditions. IPT systems ensure highly efficient battery transfer and charging. This paper presents the design and simulation of a 3.7 kW IPT system employing hybrid compensation topologies specifically inductor–capacitor–capacitor/series (LCC/S) and LCC/LCC configurations to enhance power transfer efficiency and maintain zero phase angle (ZPA) operation. The proposed system is simulated using ANSYS Maxwell and MATLAB/Simulink to evaluate voltage gain, resonant behavior, and power output under varying load conditions. The LCC/LCC topology demonstrates superior load-independent ZPA characteristics and improved receiver-side voltage stability. Simulation results confirm that both configurations achieve high efficiency and robust power transfer over an air gap of 100 mm, with the LCC/LCC system showing better tolerance to misalignment. These findings suggest that hybrid compensation topologies are viable candidates for medium-power wireless charging systems in electric vehicles and industrial automation.

Corresponding Author:

Noor Sami
Department of Electronic Engineering, College of Electronic Engineering, Ninevah University
Mosul, Iraq
Email: noor.sami.eng23@stu.uoninevah.edu.iq

1. INTRODUCTION

The belief in wireless power transfer (WPT) was initially expressed by Nikola Tesla during the 19th century. Nevertheless, WPT technology has undergone significant developments and progress over the past years. WPT technology facilitates the transmission of electromagnetic energy from a power source to an electrical load across an air gap, which makes it suitable for a wide range of applications [1]. WPT can be classified according to the distance separating the transmitter and receiver. This categorization differentiates between near-field WPT and far-field WPT. There are three primary methods for implementing WPT:

magnetically coupled WPT, electrically linked WPT, and electromagnetic radiation WPT as shown in Figure 1 [1], [2]. This paper employs magnetic coupling as a primary approach. In comparison to conventional plug-in charging, WPT technology has several advantages, including enhanced safety, increased efficiency, greater flexibility, and improved convenience [3]-[5]. Consequently, WPT technology has found extensive application in consumer electronics, electric vehicle charging, underwater power systems, implantable medical devices, portable electronics, and several industrial sectors [6]-[10]. Even though inductive power transfer (IPT) is popular in many uses because of its benefits, the challenge essential in such systems proceeds from the air-gap separating the transmitter and receiver sides that induces an inadequate coupling coefficient and major leakage. To mitigate this challenge, compensation topologies are employed as a solution to overcome the air-gap problem [11]. To facilitate high power transfer, the frequency is modulated by the power electronic converter to create a resonating connection between the inductance of the coupled coils and the added compensation capacitance [12], [13]. Among these compensation topologies own the capability to greatly moderate the volt ampere (VA) rating of the power supply, facilitate the achievement of elevated efficiencies, and enhance power transmission capacity. The double-sided LCC compensation network is the most common among high-order compensation topologies because it offers the advantages of both parallel and series compensations implemented on both the primary and secondary sides [14]-[16].

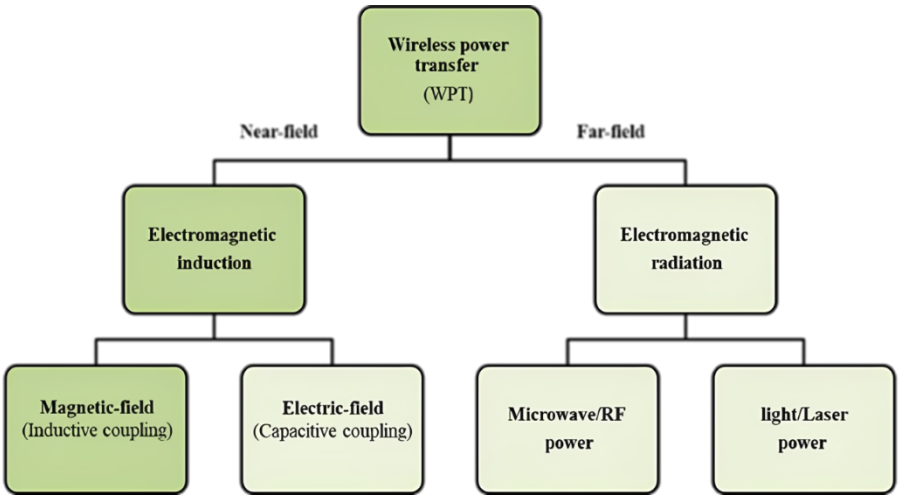

Figure 1. Classification of WPT technologies

Current research has proposed various methods for designing transactions for different topologies and applications, Bentalhik *et al.* [17]. presents design steps, efficiency metrics, experimental results, and a detailed analysis of various parameters related to WPT charger operation. The design achieves a 90% efficiency at 500 W from a laboratory prototype with specified alignment tolerances exceeding SAEJ2954 standards with the variable parameters affecting the power transfer capacity and efficiency of WPT chargers. Bouanou *et al.* [18] explores a resonant magnetic wireless charging system for electric vehicles and propose a series-series design methodology, and achieves power transmission of over 3.7 kW with an efficiency of over 90.02% and has been validated using ANSYS Maxwell and jointly simulated in ANSYS Simplorer. Lu *et al.* [19] completed a sensitivity analysis about various voltage-fed compensation frameworks within IPT systems, investigating the impact of parameter fluctuations such as load, misalignment, and efficiency on these systems, alongside experimental outcomes for 3 KW IPT systems are verified, guiding the selection of the optimal compensation network. Lu *et al.* [20] proposes a unified resonant tuning configuration that achieves constant current and voltage outputs at two operating frequencies with zero phase angle (ZPA) using a minimum number of passive components, without the need for additional power switches, the paper analysis several inductive and capacitive power transfer structures, focusing on the primary series and secondary series-parallel (S/SP) compensation topologies to demonstrate the effectiveness of the proposed approach, which improves the efficiency and regularity of wireless charging systems. Nie *et al*. [21] focus on a wireless power transmission system using an LCL network, achieving constant current and constant voltage charging through frequency modulation, effectively managing output characteristics, and maintaining performance across different loads while charging the battery.

2. PROCEDURE DESIGN OF IPT SYSTEM

A resonant inductive wireless charging method involves of two main circuits: the transmitter and the receiver, as shown in Figure 2. The transmitter circuit consists of a power supply, which is a sinusoidal alternating voltage source, a transmitter rectifier, a capacitive filter, and a full bridge inverter. It also includes the transmitter compensation network and the primary coil (LP). The receiver circuitry involves the secondary coil (LS), the receiver compensation network, the bridge rectifier, and the load, which represents a battery [15], [22]. To obtain the values of self and mutual inductances as well as the coupling coefficient through finite element analysis simulation for modeling, designing, and analyzing the IPT system using the ANSYS Maxwell tool. The design of the circular charging pads consists of a flat helical coil with ferrite and aluminum shields to protect against magnetic flux leakage. This design was realized using ANSYS Maxwell-3D, as shown in Figure 3. The design parameters were selected as shown in Table 1. The coil parameters were extracted from the finite element analysis (FEA) and used in a circuit model in ANSYS Simplorer to analyze the performance of the entire system [8], [11]. Figure 4 displays the FEA of the slackly coupled transformer. The simulation outcomes expose that the self-inductance of the primary and the self-inductance of the secondary coils are 122.777 µH and 139.953 µH, respectively, and the mutual inductance between these coils is 77.6413 µH [7], as shown in Table 2.

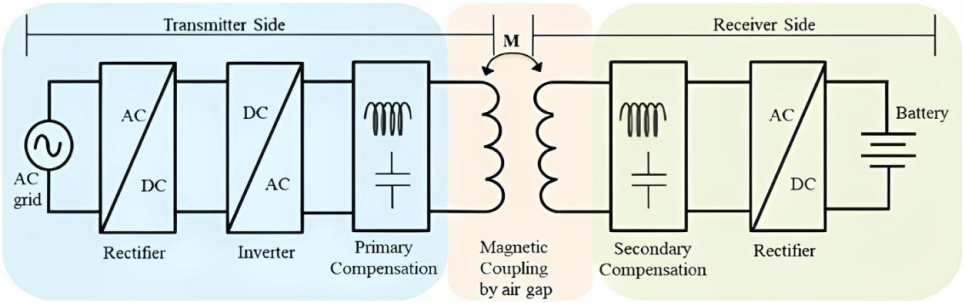

Figure 2. Block diagram of IPT system [13]

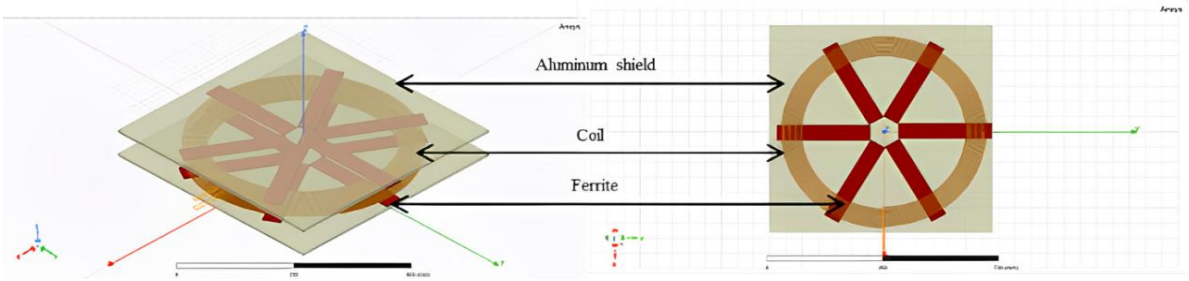

(a) (b)

Figure 3. Charging pad model in ANSYS Maxwell: (a) 3D- view and (b) top view

Table 1. Simulation design of the circular charging pad parameters

Design parameters	Value
Inner radius	250 mm
Inter-turn separation	0.1 mm
Cross-sectional area of the conductor	6.3 mm^2
No. of turns	11
Ferrites	285×50×5 mm
Aluminum shield	680×680×10 mm

Table 2. The simulation results obtained from ANSYS Maxwell

Parameters	Value
L_p	122.777 µH
L_s	139.953 µH
M	77.6413 µH
K	0.592

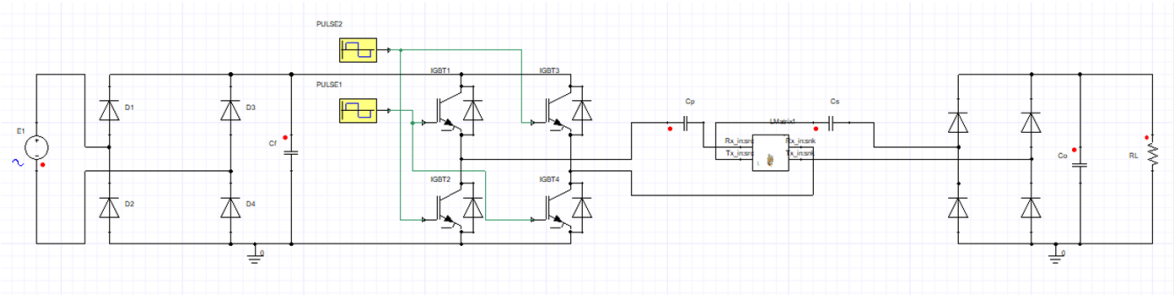

Figure 4. IPT System in ANSYS Maxwell Simplorer

3. METHOD

Compensation networks are an important component of an IPT system, reducing the system voltage rating and improving power transmission capacity. Moreover, the equivalent load of the battery differs during the charging period, affecting the input impedance value and, consequently, the performance of the entire system. Compensation topologies are of two types: basic and hybrid. There are four basic topologies based on the location of the capacitive compensation: series-series (SS), parallel-parallel (PP), parallel-series (PS), and series-parallel (SP), as shown in Figure 5. Among the four basic topologies, the SS topology is the most widely used due to its simple design and independence of the coupling coefficient (k) and load. However, its main drawback is the large current surge when the secondary circuit is suddenly closed [9]. This results in a significant increase in the induced current within the primary windings, leading to severe short circuits that damage the primary circuit. As a result, hybrid resonant compensation circuits consist of multiple passive elements, such as the LC/LC and LCC/LCC [1], [15]. These topologies are typically considered to accomplish a constant voltage output, constant current output, or both [21]. In this paper, we will discuss two types of topologies: LCC/S compensation and LCC/LCC compensation.

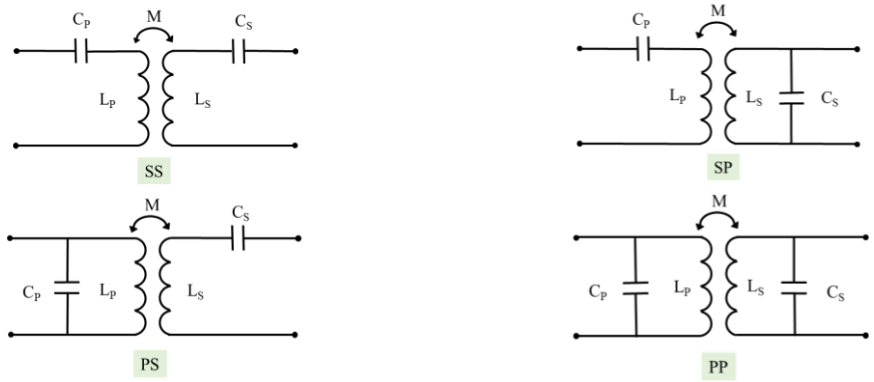

Figure 5. Basic compensation topology

3.1. Analysis of LCC/S compensation topology

Figure 6 illustrates an IPT system with an LCC/S compensation topology. V_{in} represents the AC input voltage, while V_o and I_o represent the DC output voltage and current, respectively. The high-frequency input and output voltages are represented by V_P and V_S, while I_P and I_S represent the high-frequency input and output currents. The full-bridge inverter consists of four power transistors, Q_1–Q_4, used to convert the DC voltage (V_{DC}) into a square-wave voltage. Due to the multiple harmonics generated by the inverter, fundamental harmonic analysis (FHA) is used for qualitative analysis in WPT systems [23]. L_P and L_S denote the self-inductances of the primary and secondary windings, respectively. M signifies the mutual inductance between the primary and secondary windings, which can be calculated using (1).

$$M = K\sqrt{L_P L_S} \quad (1)$$

The resonant networks consist of one inductor, L_{P1}, and three capacitors, C_{P1}, C_P, and C_S. A bridge rectifier consisting of 4 diodes, D_1 to D_4, is used to adjust the output voltage V_o to the battery charging voltage V_b, where I_o is the output current, I_b is the battery charging current, these can be calculated using the (2), and (3), C_o is the output filter capacitor, and R_L is the output load, R_o is the equivalent AC load resistance and can be calculated by (4) [4], [24].

$$V_b = \frac{\pi\sqrt{2}}{4} V_o \quad (2)$$

$$I_b = \frac{2\sqrt{2}}{\pi} I_o \quad (3)$$

$$R_o = \frac{8}{\pi^2} R_L \quad (4)$$

Figure 6 shows the circuit diagram of the LCC/S compensated topology. The IPT charging system and the compensation topology components were designed based on using (5), (6), (7), and (8) to obtain the electrical parameters.

$$\mathrm{L_{P1}} = \frac{\mathrm{V_S M}}{\mathrm{V_P}} \quad (5)$$

$$\mathrm{C_{P1}} = \frac{1}{\omega^2 \mathrm{L_{P1}}} \quad (6)$$

$$\mathrm{C_P} = \frac{1}{\omega^2 (\mathrm{L_1 - L_{P1}})} \quad (7)$$

$$\mathrm{C_S} = \frac{1}{\omega^2 \mathrm{L_2}} \quad (8)$$

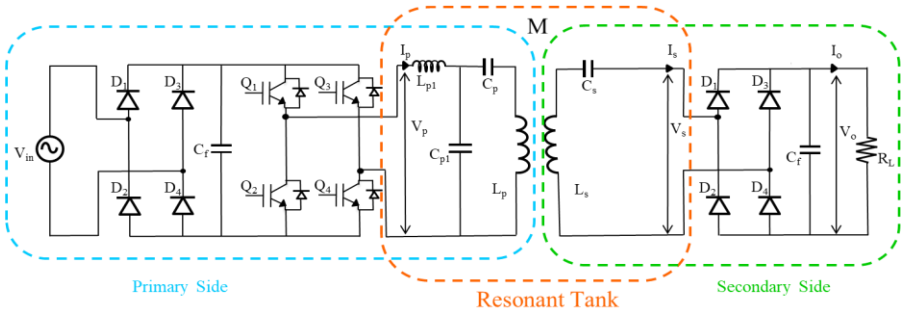

Figure 6. The circuit diagram of the LCC/S compensated topology

3.2. Analysis of LCC/LCC compensation topology

The resonant networks comprise two inductors designated as L_P and L_S, alongside four capacitors labeled C_{P1}, C_{P2}, C_P, and C_S. A bridge rectifier, consisting of four diodes identified as D_1, D_2, D_3, and D_4, is employed to regulate the output voltage V_o to align with the battery charging voltage V_b, in which I_o denotes the output current, I_b signifies the battery charging current, C_o represents the output filter capacitor, and R_L indicates the output load, as shown in Figure 7 [25]. The analytical approach is executed utilizing the FHA to investigate the wireless power transmission charging pad and to validate the electrical parameters [23]. The IPT charging system has been accurately designed, and the elements of the compensation network were designed based on using (9), (10), (11), (12), and (13) to obtain the electrical parameters.

$$L_{P1} = L_{P2} = \sqrt{R_{ac}\frac{M}{\omega}} \sqrt[4]{\frac{R_2}{R_1} + \left(\frac{R_2}{\omega M}\right)^2} \quad (9)$$

$$C_{P1} = \frac{1}{\omega^2 L_{P1}} \quad (10)$$

$$C_{P2} = \frac{1}{\omega^2 L_{P2}} \quad (11)$$

$$C_P = \frac{1}{\omega^2 (L_1 - L_{P1})} \quad (12)$$

$$C_S = \frac{1}{\omega^2 (L_2 - L_{P2})} \quad (13)$$

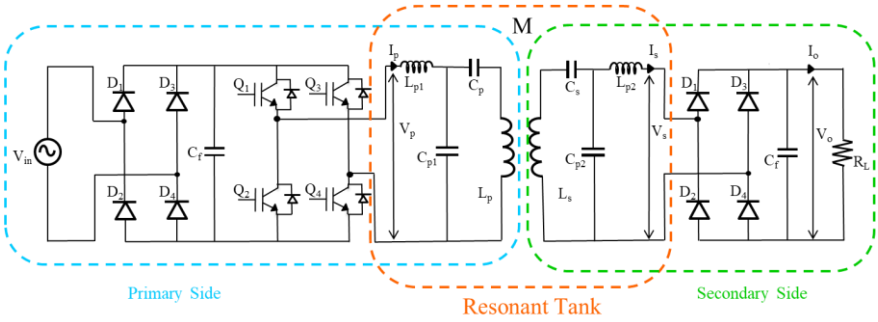

Figure 7. The circuit diagram of the LCC/LCC compensated topology

4. RESULTS AND DISCUSSION

The FEA simulation results, following the design and analysis of the wireless power transmission charging pad, and the certification of the parameters (LP, LS, M, and K) listed in Table 2. The theoretical values of the passive elements in the compensation topology can be obtained from the simulation values generated by ANSYS Maxwell-3D software using the appropriate equations. The values were computed, and a simulation of a 3.7 kW WPT1 charging system with a magnetic gap Z1 was performed in accordance with the SAEJ2954 charging standard with MATLAB/Simulation software.

4.1. LCC/S compensation result

After completing the design steps using ANSYS Maxwell-3D software and analysing the circuit for LCC/S topology, the IPT charging system and the compensation network elements were designed using (5), (6), (7), and (8) to obtain the electrical parameters, which are listed in Table 3. These capacitors are designed to operate in resonance with the primary and secondary self-inductance.

Table 3. Results of LCC/S topology

Parameters	Value
V_{in}	300 V
L_{P1}	109.353 µH
C_{P1}	32.060 nF
C_P	261.168 nF
C_S	25.050 nF
R_L	10 Ω
f	85 kHz
Z_g	100 mm

Figure 8 shows that the primary voltage (V_P), represents the output of the inverter as a square wave. In an inductive WPT system using a hybrid LCC/S compensation topology, the primary current typically exhibits a high initial value upon system startup and then gradually decreases until it extents a steady state. The LCC network is carefully designed to operate near its resonant frequency. During startup, the system may not reach resonance immediately, resulting in impedance mismatch, which causes a sudden surge in currents. As the operating frequency stabilizes at the resonant frequency, the impedance mismatch increases, causing the current to decrease to its optimal value. The secondary voltage (V_S), representing the output of the compensation circuit and the input of the bridge rectifier, is also a square wave, as shown in Figure 9. Transmission system using a hybrid LCC/S compensation topology, the primary current typically exhibits a high initial value upon system startup and then gradually decreases until it extents a steady state, as shown in Figure 8.

In addition, the primary voltage and current are in phase, like the secondary voltage and current, so the system works at a resonant frequency, and the primary and secondary current (I_P, I_S) are sine waves as shown in Figure 10. The secondary current increases because the series resonant compensation significantly reduces the impedance, facilitating a large current flow. The current maintains phase alignment with the

primary current because the LCC network on the primary side is specially designed to make the input impedance completely resistive at the operating frequency, eliminating reactive components and ensuring that the voltage and current remain in phase. Since the system operates at resonance on the primary and secondary sides, mutual coupling maintains phase alignment, resulting in phase-matched voltage and current waves on both sides. This enhances power transfer efficiency.

In an LCC/S compensated wireless power transmission system, the secondary voltage is inherently lower than the primary voltage, as shown in Figure 11, due to the winding ratio and energy conservation principles. However, both voltages maintain phase alignment responsibilities to LCC resonant compensation on the primary side and the series LCC on the secondary side, which ensures purely resistive operation at the resonant frequency, eliminating any phase shift. Figure 12 shows the load voltage and current (V_L, I_L).

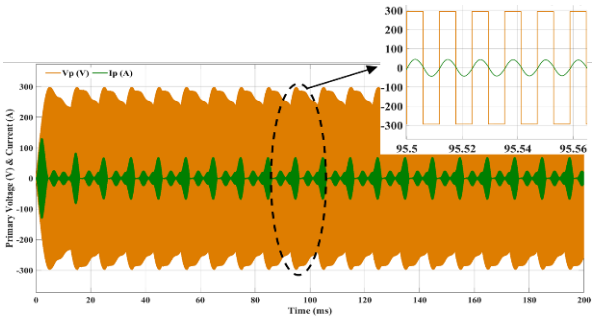

Figure 8. Output current and voltage waveforms of the inverter

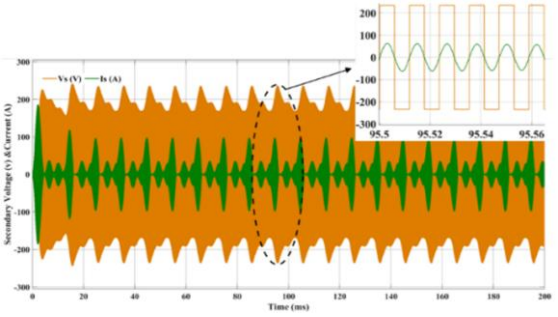

Figure 9. Current and voltage of the secondary side of the compensation network

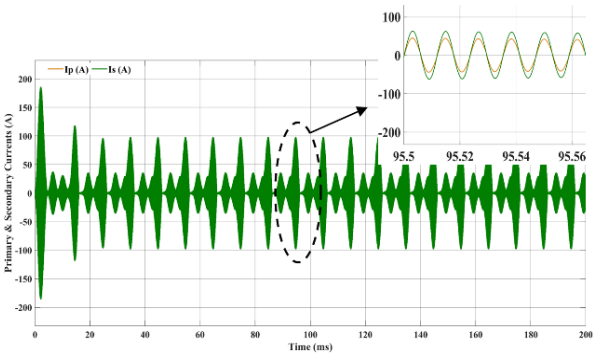

Figure 10. Primary and secondary current

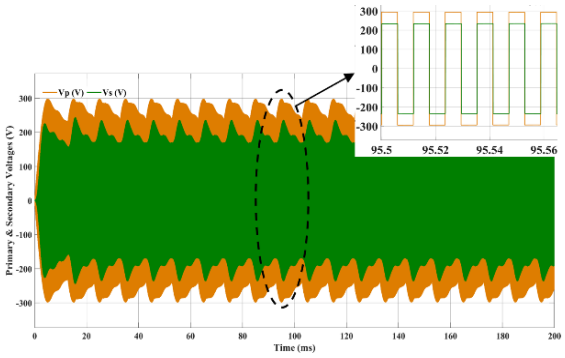

Figure 11. Primary and secondary voltage

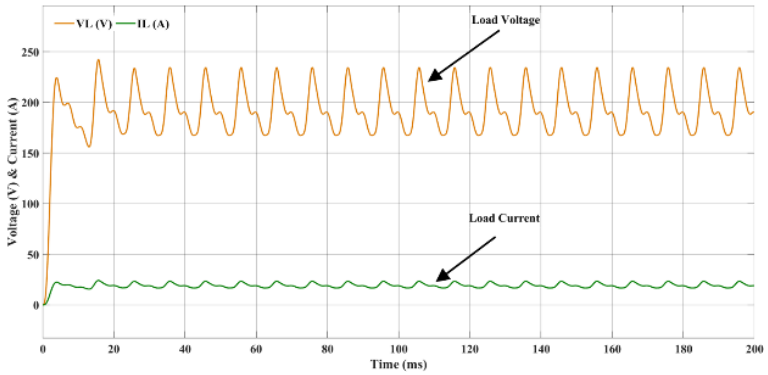

Figure 12. Current and voltage waveforms of load

4.2. LCC/LCC compensation result

Upon the completion of the design procedures utilizing ANSYS Maxwell-3D software along with the circuit analysis of the LCC/LCC topology, the elements of the IPT charging system and compensation

network were accurately formulated by applying (9), (10), (11), (12), and (13) to determine the required electrical parameters, which are specified in Table 4. In the context of the LCC/LCC topology, Figure 13 shows that the primary voltage (V_P).

The secondary voltage (V_S), representing the output of the compensation as displayed in Figure 14. Figure 15 shows that in the LCC/LCC topology for IPT, the primary current leads the secondary current due to the resonant response of the system and the power stream from the source to the load through the magnetic field. The current in the primary coil is determined by the response of the primary LCC network, while the current in the secondary coil is generated by mutual induction. In an LCC/LCC topology, a phase difference occurs between the primary and secondary currents because each terminal contains a compensation network with a different frequency response. Any deviation from ideal resonance, or a different in load or connection, results in a difference in the current response and, consequently, a phase difference. VP and VS are a square wave, as displayed in Figure 16. Furthermore, the primary current and voltage are in phase, as are the secondary voltage and currents.

Nevertheless, the system is consecutively at resonant frequency alongside with a phase shift between the primary and secondary voltages. In addition, the primary and secondary currents (I_P, I_S) are sine waves. Moreover, there is a phase-shift between the primary and secondary voltages (V_P, V_S) as shown in Figure 16. Figure 17 also shows the voltage and current load (V_L, I_L). Table 5 shows the comparison between two compensation topologies. In Table 6 shows a direct comparison between the proposed method and previous literature.

Table 4. LCC/LCC topology results

Parameter	Value	Parameter	Value
V_{in}	300 V	C_S	33.191 nF
L_{P1}, L_{P2}	34.325 µH	R_L	10 Ω
C_{P1}, C_{P2}	102.139 nF	f	85 kHz
C_P	39.636 nF	Z_g	100 mm

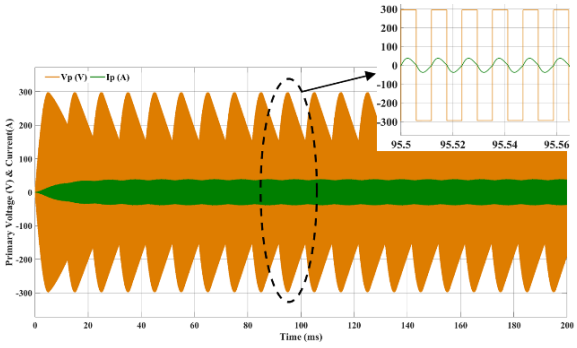

Figure 13. Output current and voltage waveforms of the inverter

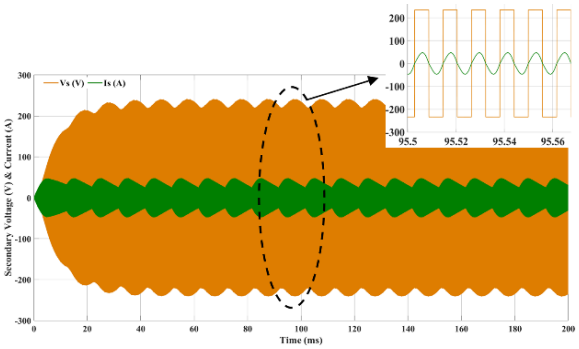

Figure 14. Current and voltage of the secondary side of the compensation network

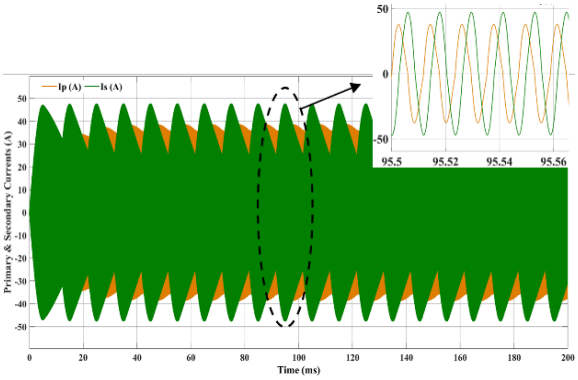

Figure 15. Primary and secondary current

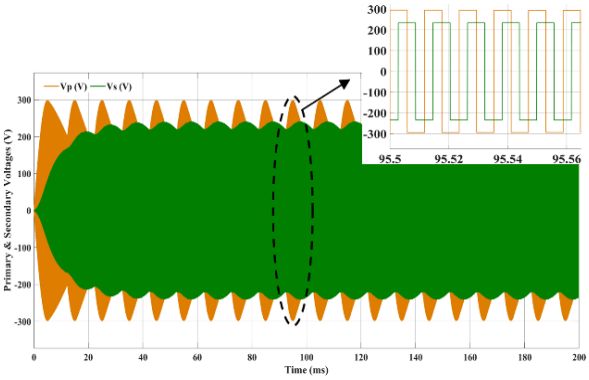

Figure 16. Primary and secondary voltage

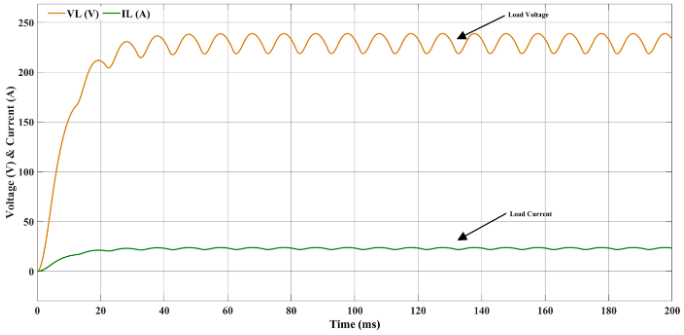

Figure 17. Current and voltage waveforms of load

Table 5. Comparison between two compensation topologies

Parameter	LCC/S	LCC/LCC
Efficiency (%)	91.8	94.1
Max transfer power (kW)	3.7	3.7
Misalignment tolerance	Moderate	Better
ZPA achieved	Yes	Yes

Table 6. Comparison between the proposed method and previous literature

Parameter	[1]	[12]	[15]	[26]	This work
Compensation topology	LCC-S	LCC-S and LCC-LCC	LCC-LCC	LCC-S	LCC-S and LCC-LCC
Simulation/hardware	Both	Both	hardware	Both	Simulation
Max power	1.5 kW	5 Kw	6.6 kW	1.85 kW	3.7 kW
Efficiency	Enhance	Enhance	Enhance	Improve	Enhance
Gap distance	-	-	-	-	100 mm

5. CONCLUSION

In this work, the performance of two hybrid compensation topologies, LCC/S and LCC/LCC was analyzed for a 3.7 kW inductive power transfer system. The simulation results confirm that both configurations can achieve ZPA operation and deliver substantial power over a moderate air gap. Among them, the LCC/LCC topology demonstrated more consistent voltage gain, better load regulation, and improved tolerance to receiver misalignment due to its inherent load-independent ZPA feature. Despite promising results, this study remains limited to simulation-based analysis. Real-world factors such as magnetic coupling variation, EMI, parasitic losses, and thermal constraints were not considered. As such, future work should include hardware prototyping, experimental efficiency validation, and advanced control strategies to dynamically adjust to varying loads and alignment conditions. Exploring bidirectional IPT, model predictive control, and renewable energy integration will further enhance the practical applicability of IPT systems in smart mobility and industrial applications. In future work, the prototypes are implemented in the next version. This work will include the construction and testing of a low-power IPT prototype using LCC/LCC or LCC/S. The future work could also be expanded by: simulating dynamic battery load and developing adaptive compensation; magnetic protection and coil optimization; investigating new ferrite configurations or Litz wire geometries to reduce leakage and loss; and optimizing coil shapes.

ACKNOWLEDGMENTS

The author would like to express his deep gratitude to Ninevah University, College of Electronics Engineering, Department of Electronic Engineering, which supported this effort.

FUNDING INFORMATION

No funding involved.

AUTHOR CONTRIBUTIONS STATEMENT

This journal uses the Contributor Roles Taxonomy (CRediT) to recognize individual author contributions, reduce authorship disputes, and facilitate collaboration.

Name of Author	C	M	So	Va	Fo	I	R	D	O	E	Vi	Su	P	Fu
Noor Sami		✓	✓		✓	✓	✓	✓	✓	✓				✓
Harith Al-Badrani	✓	✓		✓	✓	✓		✓	✓	✓	✓	✓		✓

C : **C**onceptualization
M : **M**ethodology
So : **So**ftware
Va : **Va**lidation
Fo : **Fo**rmal analysis
I : **I**nvestigation
R : **R**esources
D : **D**ata Curation
O : Writing - **O**riginal Draft
E : Writing - Review & **E**diting
Vi : **Vi**sualization
Su : **Su**pervision
P : **P**roject administration
Fu : **Fu**nding acquisition

CONFLICT OF INTEREST STATEMENT

The authors declare that they have no known computing financial interests or personal relationships that could have appeared to influence the work reported in this paper.

DATA AVAILABILITY

The data that support the findings of this study are available from the corresponding author.

REFERENCES

[1] W. Li, W. Mei, Q. Yuan, Y. Song, Z. Dongye, and L. Diao, "Detuned resonant capacitors selection for improved misalignment tolerance of LCC-S compensated wireless power transfer system," *IEEE Access*, vol. 10, pp. 49474–49484, 2022, doi: 10.1109/ACCESS.2022.3172314.

[2] Z. Xue, W. Liu, C. Liu, and K. T. Chau, "Critical review of wireless charging technologies for electric vehicles," *World Electric Vehicle Journal*, vol. 16, no. 2, p. 65, Jan. 2025, doi: 10.3390/wevj16020065.

[3] J. Yang, R. Liu, Q. Tong, X. Yang, Q. Liu, and A. Yao, "Multi-objective optimization of LCC-S-compensated IPT system for improving misalignment tolerance," *Applied Sciences*, vol. 13, no. 6, p. 3666, Mar. 2023, doi: 10.3390/app13063666.

[4] J. Yang, X. Zhang, K. Zhang, X. Cui, C. Jiao, and X. Yang, "Design of LCC-S compensation topology and optimization of misalignment tolerance for inductive power transfer," *IEEE Access*, vol. 8, pp. 191309–191318, 2020, doi: 10.1109/ACCESS.2020.3032563.

[5] M. Wu *et al.*, "A compact coupler with integrated multiple decoupled coils for wireless power transfer system and its anti-misalignment control," *IEEE Transactions on Power Electronics*, vol. 37, no. 10, pp. 12814–12827, Oct. 2022, doi: 10.1109/TPEL.2022.3166888.

[6] X. Mou, D. Gladwin, J. Jiang, K. Li, and Z. Yang, "Near-field wireless power transfer technology for unmanned aerial vehicles: a systematic review," *IEEE Journal of Emerging and Selected Topics in Industrial Electronics*, vol. 4, no. 1, pp. 147–158, Jan. 2023, doi: 10.1109/JESTIE.2022.3213138.

[7] L. Yang, Z. Geng, S. Jiang, and C. Wang, "Analysis and design of an S/PS−compensated WPT system with constant current and constant voltage charging," *Electronics*, vol. 11, no. 9, p. 1488, May 2022, doi: 10.3390/electronics11091488.

[8] G. Rituraj and P. Kumar, "A new magnetic structure of unipolar rectangular coils in WPT systems to minimize the ferrite volume while maintaining maximum coupling," *IEEE Transactions on Circuits and Systems II: Express Briefs*, vol. 68, no. 6, pp. 2072–2076, Jun. 2021, doi: 10.1109/TCSII.2020.3044585.

[9] C. Fu, D. Wang, and Q. Zhao, "A compact and coupling-smooth magnetic coupler design for AGV wireless charging application," *IEEE Access*, vol. 11, pp. 11288–11297, 2023, doi: 10.1109/ACCESS.2023.3236815.

[10] Z. Yuan *et al.*, "High-order compensation topology integration for high-tolerant wireless power transfer," *Energies*, vol. 16, no. 2, p. 638, Jan. 2023, doi: 10.3390/en16020638.

[11] J. Mai, Y. Wang, Y. Yao, M. Sun, and D. Xu, "High-misalignment-tolerant IPT systems with solenoid and double D pads," *IEEE Transactions on Industrial Electronics*, vol. 69, no. 4, pp. 3527–3535, Apr. 2022, doi: 10.1109/TIE.2021.3075841.

[12] K. K. Prasad and V. Agarwal, "Design recommendations considering charging pads' self-inductance variation with LCC–S and LCC–LCC compensation based IPT chargers in low clearance EVs," *IEEE Transactions on Transportation Electrification*, vol. 10, no. 1, pp. 1758–1770, Mar. 2024, doi: 10.1109/TTE.2023.3277103.

[13] M. T. Tran, S. Thekkan, H. Polat, D.-D. Tran, M. El Baghdadi, and O. Hegazy, "Inductive wireless power transfer systems for low-voltage and high-current electric mobility applications: review and design example," *Energies*, vol. 16, no. 7, p. 2953, Mar. 2023, doi: 10.3390/en16072953.

[14] Y. M. Y. Ameen, H. Al-Badrani, and M. N. Abdul Kadi, "Design and simulation of a high-power double-output isolated Cuk converter," *Eastern-European Journal of Enterprise Technologies*, vol. 5, no. 5 (113), pp. 30–38, Oct. 2021, doi: 10.15587/1729-4061.2021.238984.

[15] Y. Chen, H. Zhang, C.-S. Shin, C.-H. Jo, S.-J. Park, and D.-H. Kim, "An efficiency optimization-based asymmetric tuning method of double-sided LCC compensated WPT system for electric vehicles," *IEEE Transactions on Power Electronics*, vol. 35, no. 11, pp. 11475–11487, Nov. 2020, doi: 10.1109/TPEL.2020.2984712.

[16] M. Rehman *et al.*, "A Review of inductive power transfer: emphasis on performance parameters, compensation topologies and coil design aspects," *IEEE Access*, vol. 11, pp. 144978–145010, 2023, doi: 10.1109/ACCESS.2023.3344041.

[17] I. Bentalhik *et al.*, "Analysis, design and realization of a wireless power transfer charger for electric vehicles: theoretical approach and experimental results," *World Electric Vehicle Journal*, vol. 13, no. 7, p. 121, Jul. 2022, doi: 10.3390/wevj13070121.

[18] T. Bouanou, H. El Fadil, A. Lassioui, I. Bentalhik, M. Koundi, and S. El Jeilani, "Design methodology and circuit analysis of wireless power transfer systems applied to electric vehicles wireless chargers," *World Electric Vehicle Journal*, vol. 14, no. 5, p. 117, May 2023, doi: 10.3390/wevj14050117.

[19] J. Lu, G. Zhu, H. Wang, F. Lu, J. Jiang, and C. C. Mi, "Sensitivity analysis of inductive power transfer systems with voltage-fed compensation topologies," *IEEE Transactions on Vehicular Technology*, vol. 68, no. 5, pp. 4502–4513, May 2019, doi: 10.1109/TVT.2019.2903565.
[20] J. Lu, G. Zhu, D. Lin, Y. Zhang, H. Wang, and C. C. Mi, "Realizing constant current and constant voltage outputs and input zero phase angle of wireless power transfer systems with minimum component counts," *IEEE Transactions on Intelligent Transportation Systems*, vol. 22, no. 1, pp. 600–610, Jan. 2021, doi: 10.1109/TITS.2020.2985658.
[21] P. Nie, S. Xu, Z. Wang, S. Hashimoto, L. Sun, and T. Kawaguchi, "Design and implementation of a wireless power transfer system using LCL coupling network with inherent constant-current and constant-voltage output for battery charging," *Energies*, vol. 18, no. 2, p. 341, Jan. 2025, doi: 10.3390/en18020341.
[22] Y. Chen *et al.*, "Reconfigurable topology for IPT system maintaining stable transmission power over large coupling variation," *IEEE Transactions on Power Electronics*, vol. 35, no. 5, pp. 4915–4924, May 2020, doi: 10.1109/TPEL.2019.2946778.
[23] W. Wang, J. Deng, D. Chen, Z. Wang, and S. Wang, "A novel design method of LCC-S compensated inductive power transfer system combining constant current and constant voltage mode via frequency switching," *IEEE Access*, vol. 9, pp. 117244–117256, 2021, doi: 10.1109/ACCESS.2021.3105103.
[24] L. S. Salman and H. Al-Badrani, "Mathematical modeling and engineering design of multi-level inverter based on selective harmonic elimination," *Przegląd Elektrotechniczny*, vol. 98, no. 11, pp. 85–88, Nov. 2022, doi: 10.15199/48.2022.11.14.
[25] J. Yan, M. J. B. A. Aziz, N. R. N. Idris, and T. Sutikno, "A single-stage constant-power and optimal-efficiency double-sided LCC wireless battery charger," *International Journal of Power Electronics and Drive Systems (IJPEDS)*, vol. 16, no. 2, p. 1409, Jun. 2025, doi: 10.11591/ijpeds.v16.i2.pp1409-1416.
[26] C.-H. Jo and D.-H. Kim, "Novel compensation parameter design methodology and maximum efficiency tracking control strategy for inductive power transfer system," *IEEE Access*, vol. 10, pp. 56133–56144, 2022, doi: 10.1109/ACCESS.2022.3178185.

BIOGRAPHIES OF AUTHORS

Noor Sami received the B.Sc. degree from the Computer and Information Department, at the College of Electronics Engineering, Ninevah University, Mosul, Iraq, in 2013. She is currently pursuing the M.Sc. degree in Electronic Engineering at Ninevah University. Her research interests include power electronic. She can be contacted at email: noor.sami.eng23@stu.uoninevah.edu.iq.

Harith Al-Badrani received the B.Sc. and M.Sc. degrees in electrical engineering from Northern Technical University, Mosul, Iraq, in 2003 and 2006, respectively, and the Ph.D.-Ing. degree in power electronics and electrical drives from the Department of Electrical Engineering and Computer Science, University of Siegen, Germany, in 2018. He is currently working as an assistant professor and a head of Electronic Dept. at the College of Electronics Engineering, Ninevah University, Mosul, Iraq. His research interests focus on power electronics and electrical drives. He can be contacted at email: harith.mohammed@uoninevah.edu.iq.